

Figure 36: Comparison of F-B least squares and tapered Yule-Walker spectral estimates for the AR(4) process.

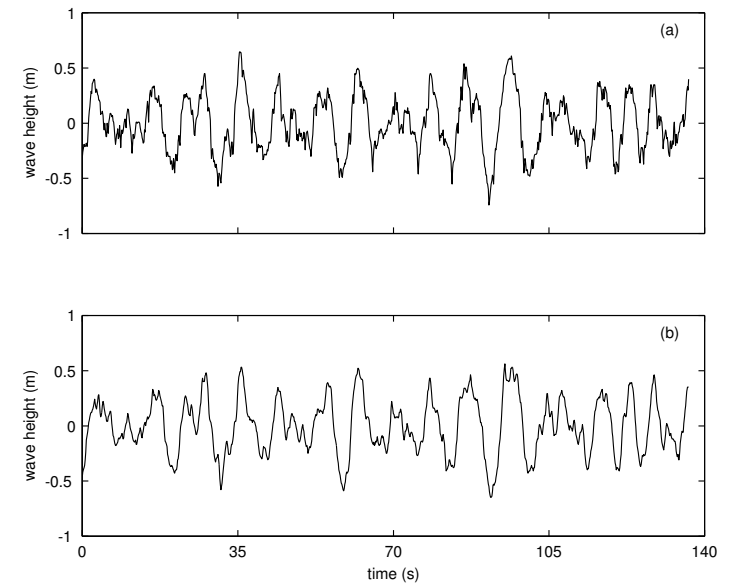


Figure 37: Simultaneous measurements of ocean waves versus time by two instruments of quite different design, (a) an infrared wave gauge, and (b) a wire wave gauge. There are  $N = 1024$  data values in each series and the sample interval is  $\delta_t = 4/30$ s. (These series were derived from data supplied courtesy of Andy Jessup, Applied Physics Lab, University of Washington.)

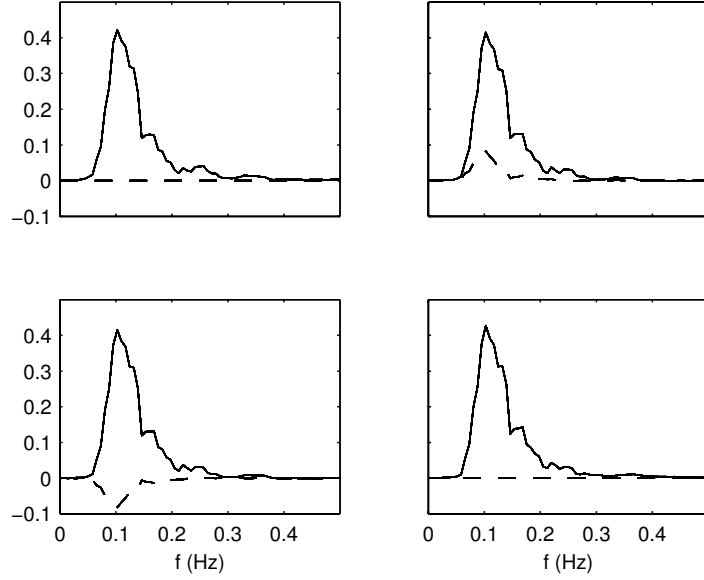


Figure 38: The estimated spectral matrix,  $\hat{\mathbf{S}}(\cdot)$ , for the two ocean wave time series. The real and imaginary parts of  $\hat{S}_{X_l X_m}(\cdot)$ ,  $l, m = 1, 2$ , are shown by solid and dashed lines, respectively.

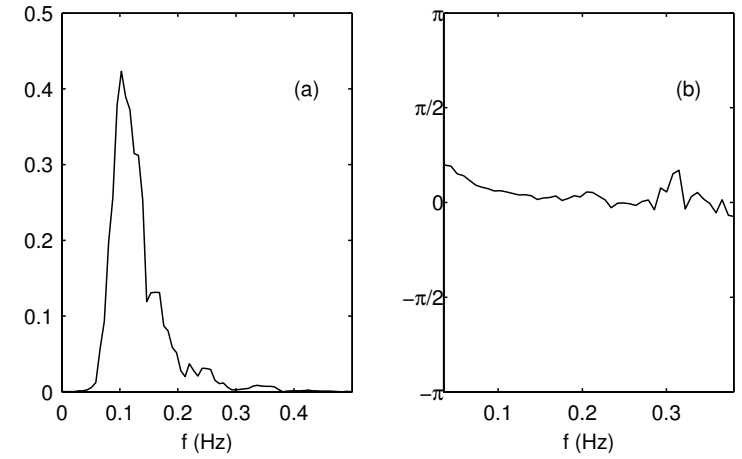


Figure 39: (a) Estimated cross-amplitude spectrum  $|\hat{S}_{X_1 X_2}(\cdot)|$ , in the interval  $[0, 0.5]$  Hz and (b) estimated phase spectrum  $\hat{\theta}_{X_1 X_2}(\cdot)$ , in the interval  $[0.035, 0.38]$  Hz, for the two ocean wave time series .

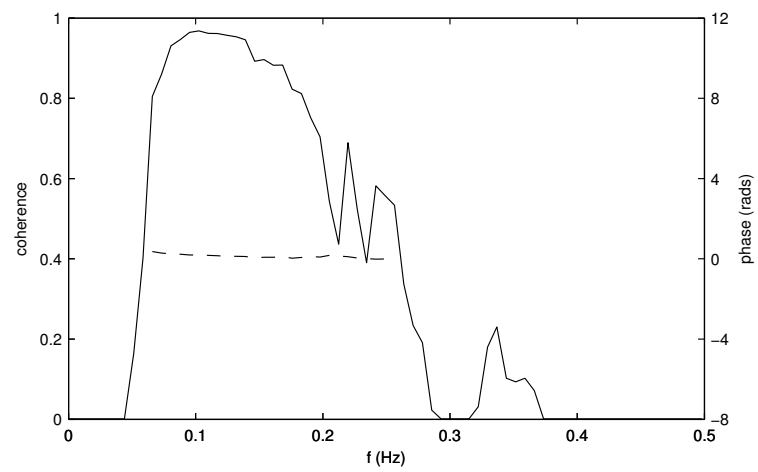


Figure 40: Coherence estimate for the two ocean wave time series. Also shown (dashed line) is the estimated phase  $\hat{\theta}_{X_1 X_2}(f)$  over frequencies for which the estimated ordinary coherence exceeds 0.5.